

## Tetrahedral Crosslinking of Dia-type Nets into Zeolitic GIS-type Framework for Optimizing Stability and Sorption

Yan-Xi Tan,<sup>a</sup> Yanan Si,<sup>a,b</sup> Wenjing Wang<sup>a</sup> and Daqiang Yuan<sup>\*,a</sup>

<sup>a</sup> State Key Laboratory of Structural Chemistry, Fujian Institute of Research on the Structure of Matter, Chinese Academy of Sciences, Fuzhou, 350002, Fujian, China. E-mail: ydq@fjirsm.ac.cn

<sup>b</sup> University of the Chinese Academy of Sciences, Beijing, 100049, China.

### 1. Materials and general methods

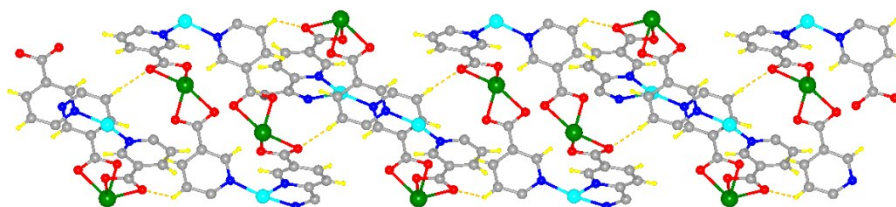


Fig. S1. Hydrogen bonds between adjacent diamondoid cages.

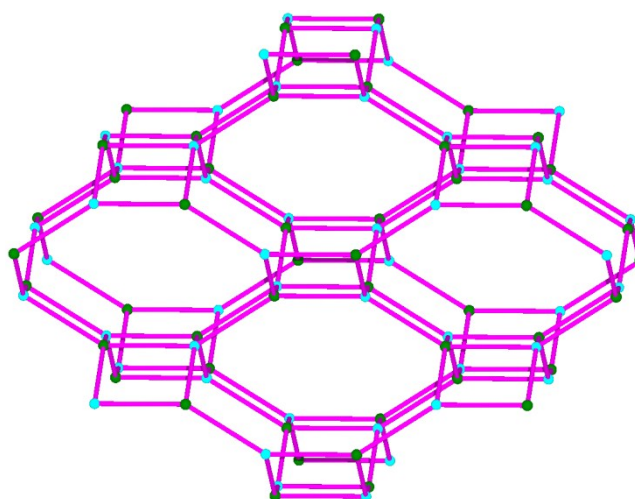


Fig. S2. GIS topology of FJI-Y3.

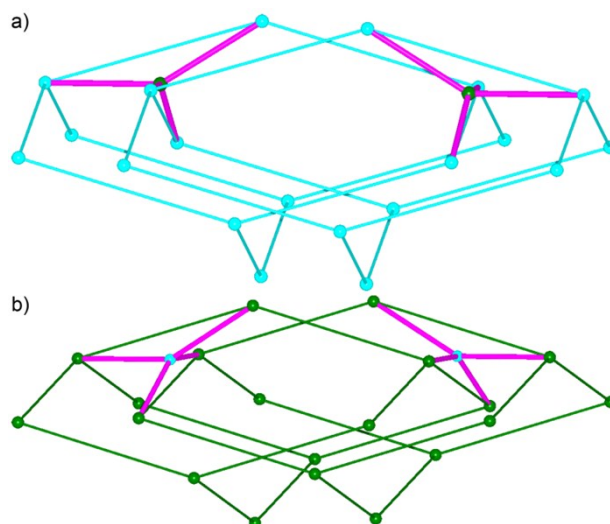


Fig. S3. Tetrahedral crosslinking of 4-fold interpenetrating *dia*-type nets.

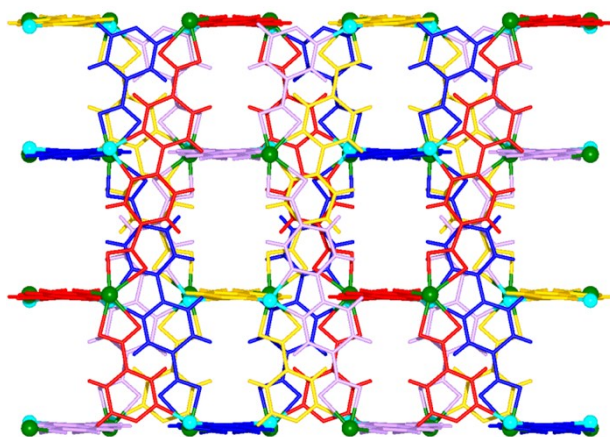


Fig. S4. The 3D interpenetrating framework of **FJI-Y3** viewing along *a* or *b* axis.

## 2. TGA curves

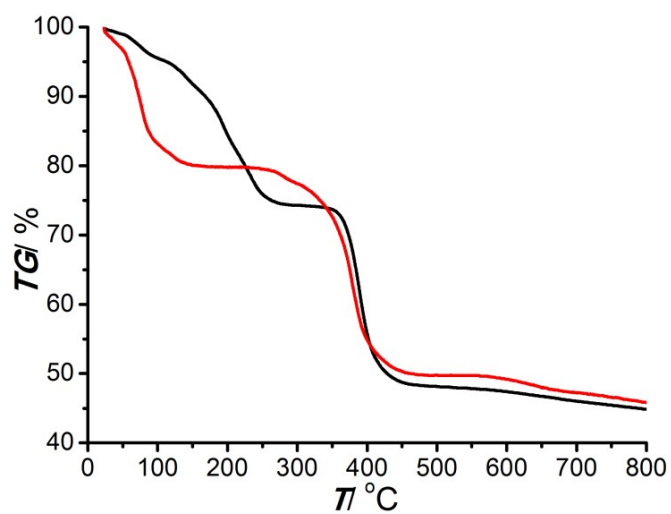


Fig. S5. TGA curves of as-synthesized **FJI-Y3** (black line) and MeOH-exchanged **FJI-Y3** (red line) samples.

### 3. Sorption isotherms

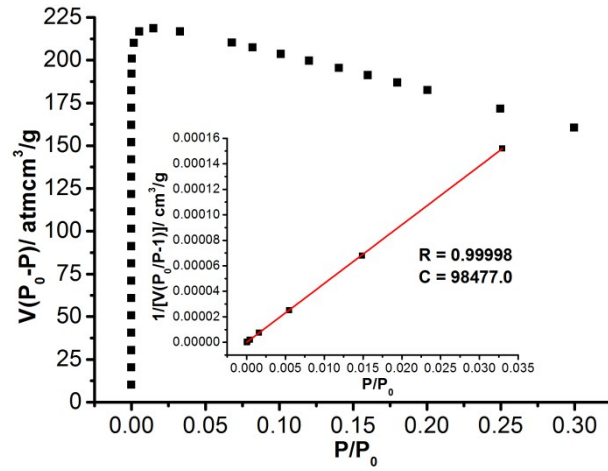


Fig. S6. BET surface area plot for FJI-Y3-ht.

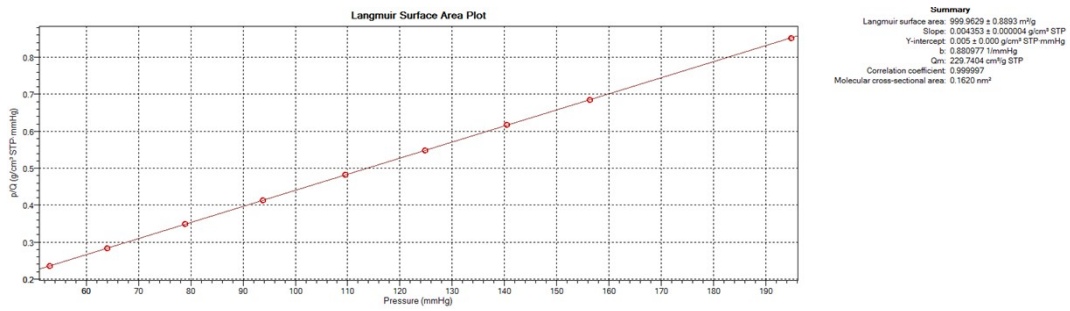


Fig. S7. Langmuir surface area plot for FJI-Y3-ht.

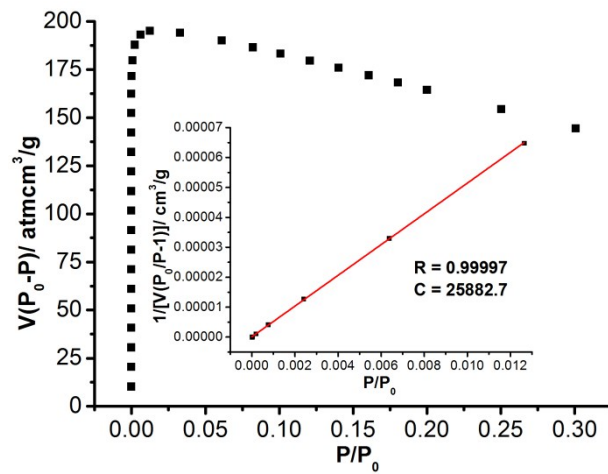


Fig. S8. BET surface area plot for FJI-Y3-ht'.

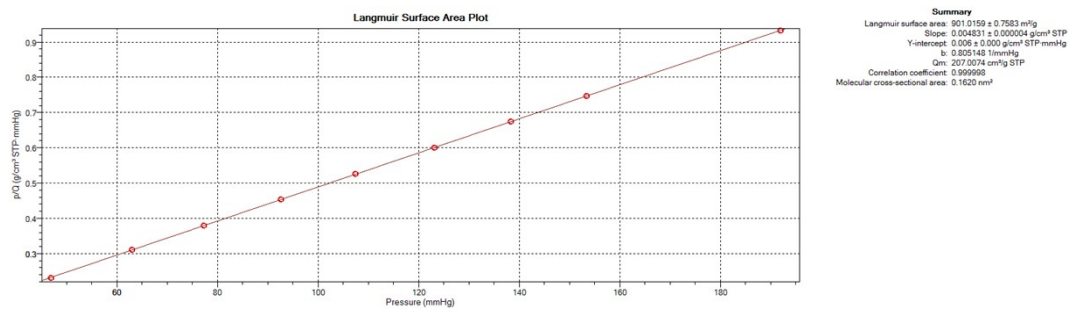


Fig. S9. Langmuir surface area plot for **FJI-Y3-ht**.

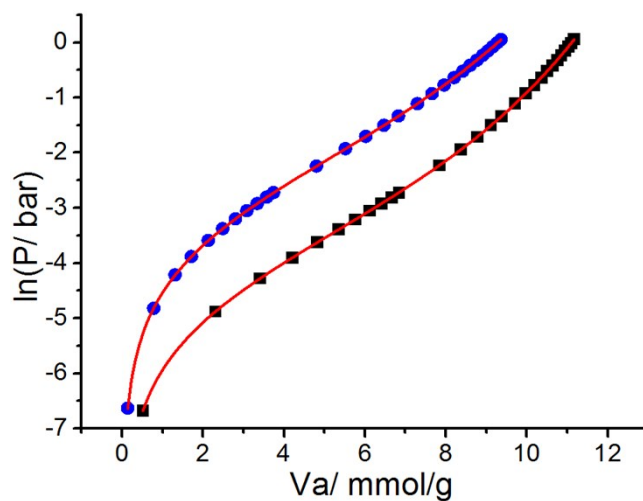


Fig. S10. D<sub>2</sub> adsorption isotherms under 77 (black) and 87 K (blue) for **FJI-Y3-ht** fitting by virial method.

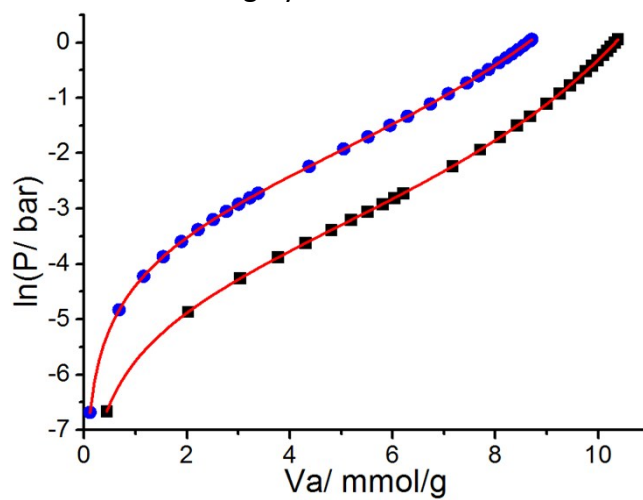


Fig. S11. H<sub>2</sub> adsorption isotherms under 77 (black) and 87 K (blue) for **FJI-Y3-ht** fitting by virial method.

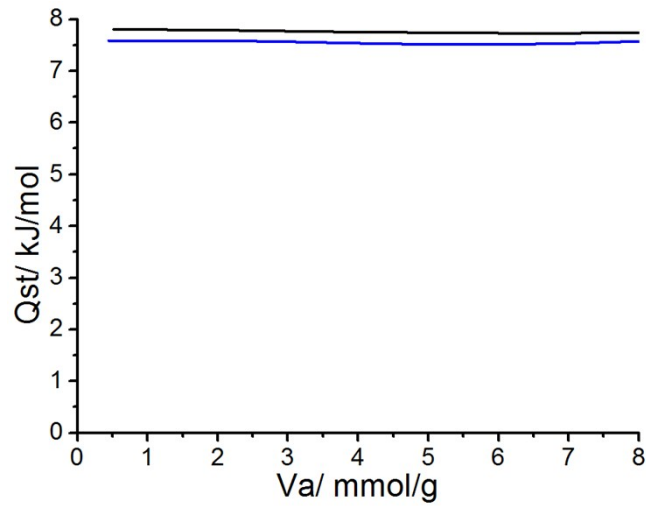


Fig. S12. The isosteric heat of D<sub>2</sub> (black) and H<sub>2</sub> (blue) adsorption for **FJI-Y3-ht** estimated by the virial equation.

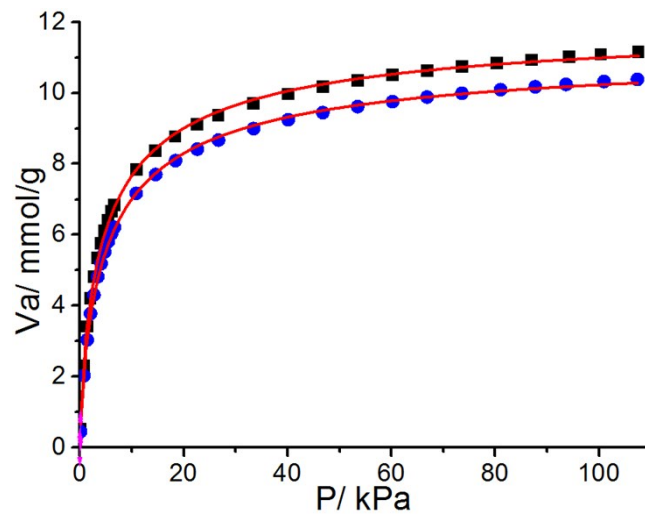


Fig. S13. Adsorption isotherms of D<sub>2</sub> (black) and H<sub>2</sub> (blue) for **FJI-Y3-ht** under 77 K. Solid lines through the experimental data are fits to the single-site L-F model.

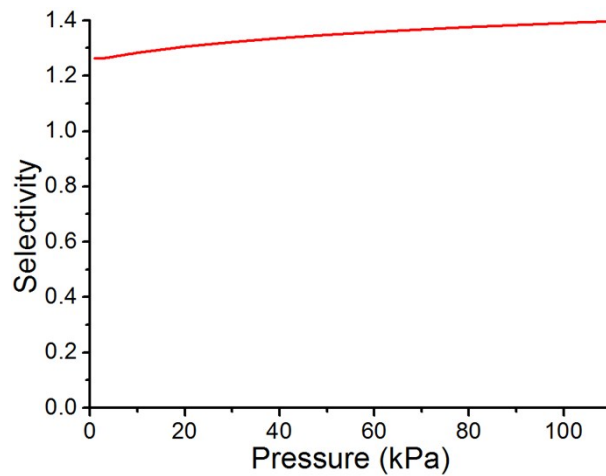


Fig. S14. Selectivity of D<sub>2</sub>/H<sub>2</sub> for **FJI-Y3-ht** under 77 K.

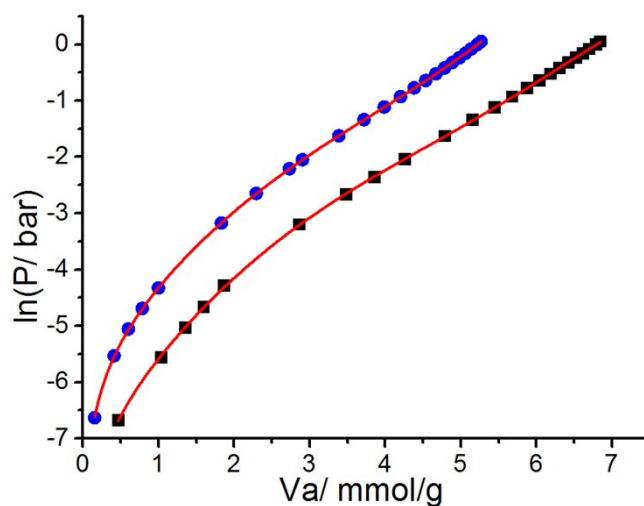


Fig. S15.  $C_2H_2$  adsorption isotherms under 273 (black) and 298 K (blue) for **FJI-Y3-ht** fitting by virial method.

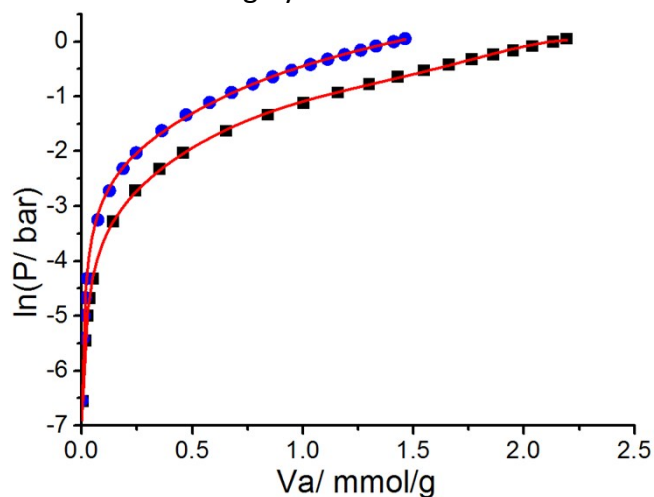


Fig. S16.  $CH_4$  adsorption isotherms under 273 (black) and 298 K (blue) for **FJI-Y3-ht** fitting by virial method.

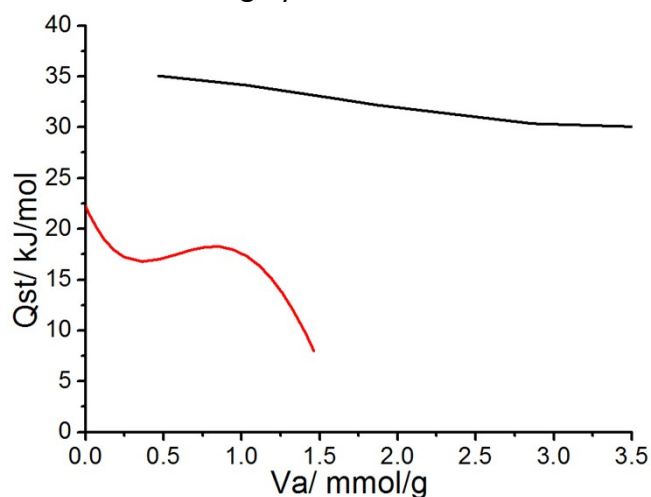


Fig. S17. The isosteric heat of  $C_2H_2$  (black) and  $CH_4$  (blue) adsorption for **FJI-Y3-ht** estimated by the virial equation.

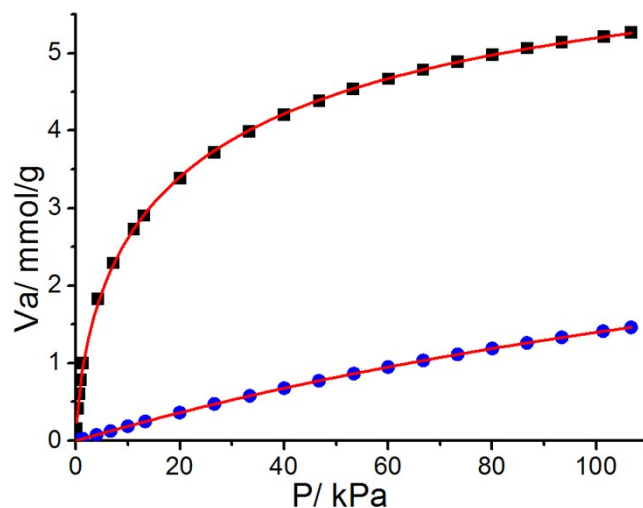


Fig. S18. Adsorption isotherms of C<sub>2</sub>H<sub>2</sub> (black) and CH<sub>4</sub> (blue) for **FJI-Y3-ht** under 298 K. Solid lines through the experimental data are fits to the single-site L-F model.

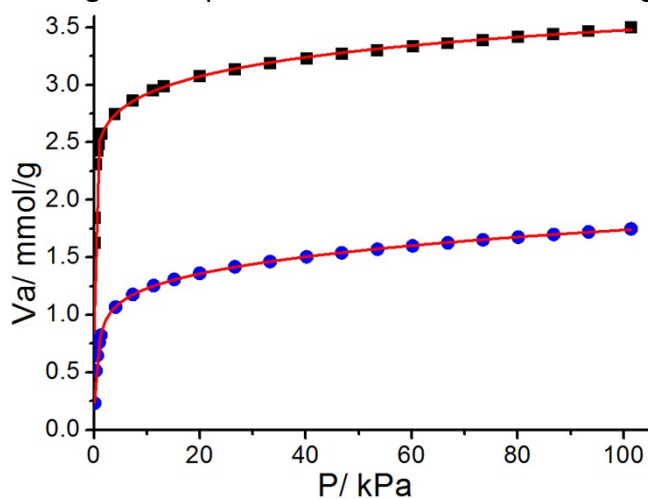


Fig. S19. Adsorption isotherms of *n*-C<sub>4</sub>H<sub>10</sub> (black) and *i*-C<sub>4</sub>H<sub>10</sub> (blue) for **FJI-Y3-ht** under 298 K. Solid lines through the experimental data are fits to the dual-site L-F model.